Model-Independent Beam Dynamics Analysis

J. Irwin, C. X. Wang, Y. T. Yan, K. L. F. Bane, Y. Cai, F.-J. Decker, M. G. Minty, G. V. Stupakov, and F. Zimmermann
Stanford Linear Accelerator Center, P.O. Box 4349, Stanford, California 94309
(Received 4 November 1998)

Using a singular value decomposition of a beam line matrix, composed of many beam position measurements for a large number of pulses, together with the measurement of pulse-by-pulse beam properties or machine attributes, the contributions of each variable to the beam centroid motion can be identified with a greatly improved resolution. The eigenvalues above the noise floor determine the number of significant physical variables. This method is applicable to storage rings, linear accelerators, and any system involving a number of sources and a larger number of sensors with unknown correlations. Applications are presented from the Stanford Linear Collider. [S0031-9007(99)08510-5]

PACS numbers: 29.27.Bd, 41.75.–i

A novel model-independent technique in particle orbit analysis is presented. In most accelerators, beam position monitors (BPMs) are used to record the transverse position, or displacement, of the centroid motion of the particle beam. For bunched beams, these displacements may be detected on a pulse-by-pulse basis. The measured displacement is a superposition of the unperturbed displacement and contributions arising from variables affecting the motion of the beam centroid. Ideally one would like to identify and remove these perturbative errors which often lead to an increased phase space occupied by the beam and, in case of a collider, can reduce the reaction rate (luminosity) at the collision point. Using multiple BPMs where the number exceeds the number of changing physical variables affecting the beam, the ability to identify these variables is greatly enhanced by taking advantage of the inherent correlations between same-pulse BPM readings. In this paper we describe techniques to enumerate and localize the variables' effect on the beam centroid motion.

For a sequence of M BPMs for P detected pulses, a matrix $B(P,M)$ can be constructed, for example, with the pth row vector $\vec{b}_p \equiv (b_p^1, b_p^2, \ldots, b_p^M)$, representing the measured trajectory of a given pulse. The actual particle trajectory may be Taylor expanded about the nominal trajectory in terms of relative deviations. Since the unperturbed particle trajectory is of no subsequent relevance, we subtract out the average terms in the series expansion to obtain

$$\vec{b}_p - \langle\vec{b}\rangle = \sum_s (\Delta\upsilon_p^s - \langle\Delta\upsilon^s\rangle)\frac{\partial\vec{b}}{\partial\upsilon^s} + \frac{1}{2}\sum_{r,s}(\Delta\upsilon_p^r\Delta\upsilon_p^s - \langle\Delta\upsilon^r\Delta\upsilon^s\rangle)\frac{\partial^2\vec{b}}{\partial\upsilon^r\partial\upsilon^s} + \cdots + \vec{n}_p\,, \quad (1)$$

where $\langle\,\rangle$ denotes an average over pulses, $\Delta\upsilon_p^s$ is the variables' difference from some nominal value for the pth pulse due to a variation indexed by s, and $\vec{n}_p$ is the contribution from random BPM noise. The variables $\Delta\upsilon^s$ can be known or unknown. They can be actual sources (a kicker voltage, magnet ripple, or klystron phase) or can be taken to be the effects of actual sources through initial beam parameters (horizontal and vertical position and slope, charge per bunch, energy or phase, or any other property of the initial phase distribution). They could also be hypothesized sources or effects thereof, such as some property of the longitudinal distribution in an upstream damping ring, or they could be a variable which is to be purposely modulated. No assumptions need be made on the statistical properties of the sources other than the fact that they be independent. If they are dependent, one or more of the chosen sources is redundant and can be removed.

A correlation in the BPM readings that might result from a common voltage they each see would be considered as arising from a physical variable. The stochastic variation in the BPM reading from a reading that would properly represent the beam position is included in the noise term $\vec{n}_p$ of Eq. (1), and is not represented as a variable. The separation of BPM noise from other variables is described below.

We define dimensionless temporal unit vectors, $\vec{q}^s$ or $\vec{q}^{r,s}$, with their pth elements ($p \in \{1,2,\ldots,P\}$) given by $q_p^s \equiv (\Delta\upsilon_p^s - \langle\Delta\upsilon^s\rangle)/[\mathrm{std}(\Delta\upsilon^s)\sqrt{P}\,]$ or $q^{r,s} \equiv (\Delta\upsilon_p^r\Delta\upsilon_p^s - \langle\Delta\upsilon^r\Delta\upsilon^s\rangle)/[\mathrm{std}(\Delta\upsilon^r\Delta\upsilon^s)\sqrt{P}\,]$, and the corresponding spatial vectors $\vec{f}_s$ or $\vec{f}_{r,s}$, given by $\vec{f}_s \equiv \mathrm{std}(\Delta\upsilon^s)\partial\vec{b}/\partial\upsilon^s$ or $\vec{f}_{r,s} \equiv \frac{1}{2}\mathrm{std}(\Delta\upsilon^r\Delta\upsilon^s)\partial^2\vec{b}/\partial\upsilon^r\partial\upsilon^s$, where std is the standard deviation over the P pulses. Note that the spatial vectors (patterns) have the dimension of length, the same as the BPM readings. Merging the double indices (r,s) into the single one(s) and letting $\hat{\vec{n}}_p \equiv (\vec{n}_p/\sqrt{P}\,)$, Eq. (1) is then reexpressed as

$$\hat{\vec{b}}_p \equiv \frac{\vec{b}_p - \langle\vec{b}\rangle}{\sqrt{P}} = \sum_s q_p^s\vec{f}_s + \hat{\vec{n}}_p\,,$$

which in matrix form is given by

$$\hat{\mathrm{B}} = QF^T + \hat{\mathrm{N}}. \quad (2)$$

If a subset of the temporal patterns (a submatrix of Q denoted by Q_s) is independently measured and is

 0031-9007/99/82(8)/1684(4)$15.00

uncorrelated to temporal patterns outside this subset, then the corresponding spatial patterns (a submatrix of F denoted by F_s) may be determined. Denoting the temporal correlation matrix $C_s \equiv Q_s^T Q_s$, then

$$F_s^T = C_s^{-1} Q_s^T \hat{\mathrm{B}} - C_s^{-1} Q_s^T \hat{\mathrm{N}}. \tag{3}$$

Note that the error term, $C_s^{-1} Q_s^T \hat{\mathrm{N}}$, arising from the BPM random noise, is reduced to $\sigma/\sqrt{P}$ because $\sum_{p=1}^{P} q_p^s \hat{n}_p^m \sim \sigma/\sqrt{P}$. This term can be further reduced as described later.

By independently measuring the temporal vectors (patterns) of the known physical changes, the various contributions to the beam centroid motion can be uniquely determined from Eq. (3). In practice, however, the particle orbit may be affected by unidentified physical variables. In this case, a singular value decomposition (SVD) [1] of the matrix $\hat{\mathrm{B}}$ given by

$$\hat{\mathrm{B}} = U \Lambda V^T \tag{4}$$

can be invoked to aid in the identification of these unknown variables. Here U and V are two orthonormal matrices and Λ is a diagonal matrix containing the eigenvalues. The eigenvectors in U and the eigenvectors in V form two complete bases, respectively, for the temporal space and the spatial space spanned by the underlying physical changes. In this representation, the number of eigenvalues above the noise floor of the eigenvalue spectrum determines the number of significant physical variables that are changing and affecting the beam centroid motion. In typical applications, there are only a few significant eigenvalues. Note that each of the eigenmodes in Eq. (4) does not correspond uniquely to the physical patterns in Eq. (2).

We next present an analysis of experimental data from the Stanford Linear Accelerator. We perform an SVD for horizontal beam centroid data consisting of $M = 130$ sequential BPMs and $P = 5000$ pulses. Figure 1 shows the spatial eigenvectors corresponding to the six largest eigenvalues. Erratic BPMs may be quickly identified as seen by the fifth and sixth subplots. Figure 2 shows the eigenvalue distribution. With the exception of the prominent eigenvalues, the distribution from BPM noise gets flatter as P becomes larger until reaching the inherent distribution of the BPM resolutions. The average of the noise-floor eigenvalues relative to the prominent ones decreases as $(1/\sqrt{M})$ times the BPM resolution. Note that, in the Stanford Linear Collider (SLC), a few BPMs are a special low-resolution type, leading to the unusually small eigenvalues from mode 126 to 130. The upward deviation of eigenvalues below mode 15 should be taken as a hint to the possible presence of "signals" in these modes. The "noise floor" is typical of all our data sets and simulations and provides us a vehicle to separate noise from signal. The persistence of spatial eigenvectors in sequential data sets is also a strong test to discriminate signals from noise.

To suppress the random errors, one may replace the Λ in Eq. (4) by $\underline{\Lambda}$ in which eigenvalues in the noise floor are set to zero, obtaining a cleaner beam line matrix $\underline{\hat{\mathrm{B}}}$. Using $\underline{\hat{\mathrm{B}}}$ in Eq. (3), one would obtain $F_s^T = C_s^{-1} Q_s^T \underline{\hat{\mathrm{B}}}$ with an error due to random BPM noise on the order of $\sigma\sqrt{D/PM}$ because only D ($\ll M$) degrees of freedom are retained [$\sum_{p=1}^{P} q_p^s \hat{n}_p^m$ is now $\sim(\sigma/\sqrt{P})\sqrt{D/M}$].

With knowledge of the number of physical variables affecting the beam motion, one can identify the location where each of these variables begins to affect the beam. We perform a sequence of SVDs on subsets of the first m BPMs in the beam line matrix, incrementing m from 7 to M. An example, which we call a degree-of-freedom plot, is shown in Fig. 3. Bad BPMs have been removed from the data sample as well as the noise floor as described previously. The curves connect the singular values in order of decreasing eigenvalue amplitude; for example, the top curve gives the largest eigenvalue obtained in each

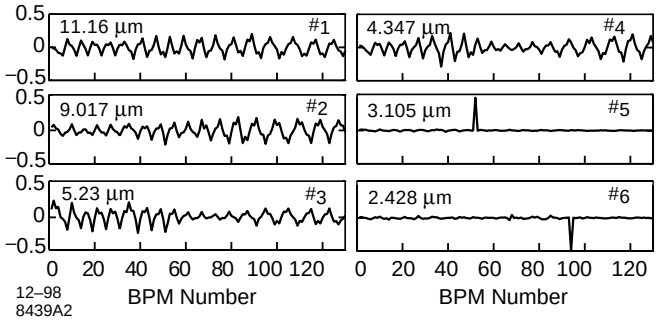

FIG. 1. Eigenvectors (unit length) corresponding to the six largest eigenvalues. The #1 and #2 plots show the two largest eigenmodes which are principally from betatron motion. The #5 and #6 plots show two bad BPMs. The associated singular values are shown in the upper-left corners. They have been normalized by a factor of $1/\sqrt{M}$.

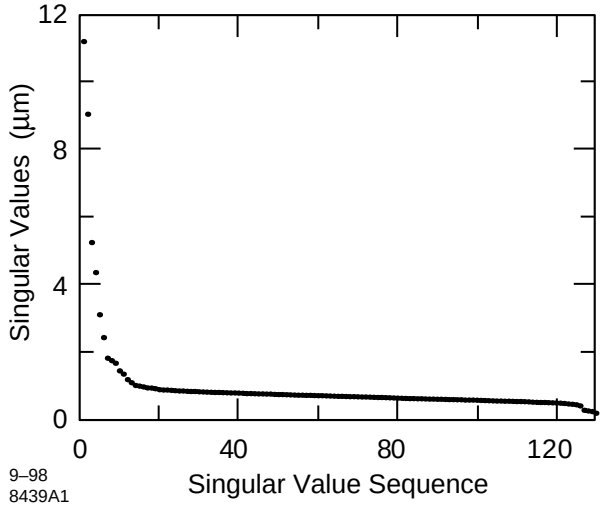

FIG. 2. Typical eigenvalue distribution from a singular value decomposition of a set of SLAC linac horizontal motion data of 5000 pulses and 130 BPMs.

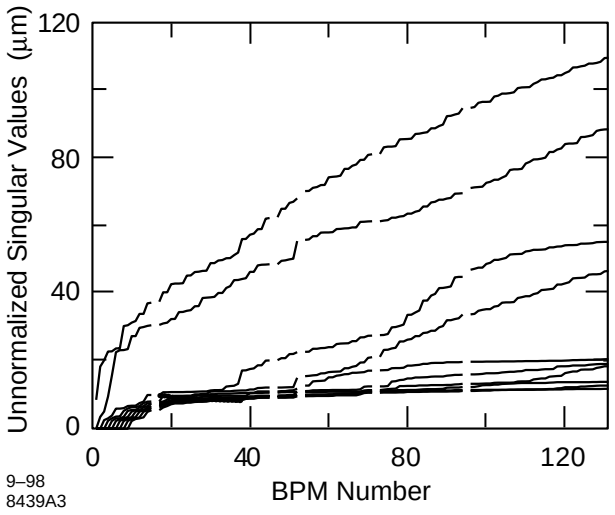

FIG. 3. Degree-of-freedom plot obtained from performing SVDs of the beam line BPM matrix subsets of an increasing number of BPMs. The eigenvalues plotted are not normalized by $1/\sqrt{M}$. The coherent signal curves grow with the number of BPMs and the slopes of the curves indicate the local strength of signals.

SVD analysis. A change in slope localizes the addition of a new perturbation. Up to BPM number 30, only two eigenvalues are evident indicating that only two variables significantly contribute to the particle trajectory up to that point in the accelerator. At about the 38th BPM an additional variable begins to affect the beam.

The two largest eigenmodes (corresponding to the two largest eigenvalue curves in Fig. 3) are principally from betatron motion but can be mixed with additional degrees of freedom. In order to find the two betatron spatial patterns for the entire BPM set, one must first determine the two betatron temporal patterns. This may be accomplished by performing an SVD of the beam line matrix for the first n BPMs, i.e., $\underline{\hat{\mathrm{B}}}_n = U_n \Lambda_n V_n^T$. Here n is chosen about equal to 7, large enough to have a meaningful SVD yet small enough so that there is little mixture of the betatron modes with additional degrees of freedom. The first two columns of U_n, to be called Q_2, define the betatron temporal patterns. Assuming weak correlation of the betatron temporal patterns with other changing physical variables (a suspect assumption), then by applying Eq. (3), one obtains $F_2 = (Q_2^T Q_2)^{-1} Q_2^T \underline{\hat{\mathrm{B}}}$, where F_2 is an $M \times 2$ matrix containing the two betatron spatial roots, $\vec{f}_1$ and $\vec{f}_2$. Instead of assuming a lack of correlation between the betatron motion and other physical variables, one can form a matrix of all measured variables, Q_s, with the Q_2 patterns included. Now $F_s = (Q_s^T Q_s)^{-1} Q_s^T \underline{\hat{\mathrm{B}}}$ will yield a better estimate of the betatron pattern. An excellent betatron pattern of either phase can be identified by purposefully modulating an upstream corrector while taking data for the beam line matrix, B, and including this modulation as a source in Q_s.

We can now complement the degree-of-freedom plot by calculating the deviation of other measured patterns from the betatron oscillations as defined by the betatron spatial patterns. If a spatial pattern $\vec{g}$ is pure betatron motion, then it can be expressed as a linear combination of the two roots $\vec{f}_1$ and $\vec{f}_2$. In general, $\vec{g} = \alpha_1 \vec{f}_1 + \alpha_2 \vec{f}_2 + \vec{d}$, where $\vec{d}$ represents a deviation from the pure betatron motion. To locate where deviations arise and to quantify their strengths, we consider all sets of three consecutive BPMs so that for each set there are three components in each of $\vec{g}$, $\vec{f}_1$, and $\vec{f}_2$, requiring the first two components of $\vec{g}$ to fit the betatron roots; the third component will have a displacement of magnitude $d = (\vec{f}_1 \times \vec{f}_2) \cdot \vec{g} / (\vec{f}_1 \times \vec{f}_2) \cdot \vec{e}_3$. Note that $\vec{e}_3 \equiv (0, 0, 1)$ is a unit vector of the third component.

Figure 4 shows two displacement plots (a-2, b-2) and their corresponding spatial patterns (a-1, b-1) for random bunch length (a-1, a-2) and phase (b-1, b-2) variations, respectively. For this case, the beam line matrix was obtained from computer simulations. Structure misalignment of 300 μm was purposely imposed at two locations. Since the wakefield effect is sensitive to bunch length changes, the displacement plot (a-2) clearly illustrates the locations and strengths of the displacements due to the two structure misalignments. On the other hand, since the wakefield effect is not sensitive to incoming phase changes, no evidence is seen for displacement in (b-2).

Structure misalignments which cause transverse deflecting wakefields have been experimentally investigated and analyzed. We measured the temporal patterns of the beam current for three consecutive sets of 5000-pulse data: nominal conditions (set D1), same as D1 but with five correctors used to make a local closed bump in the single-particle trajectory (set D2), and nominal conditions again (set D3). The effect of the bump on the particle trajectory (including collective effects) is shown in Fig. 5(a). The difference orbits D2 − D1 are shown as a solid curve and D2 − D3 as dots. The good agreement of the difference orbits indicates a high degree of reproducibility.

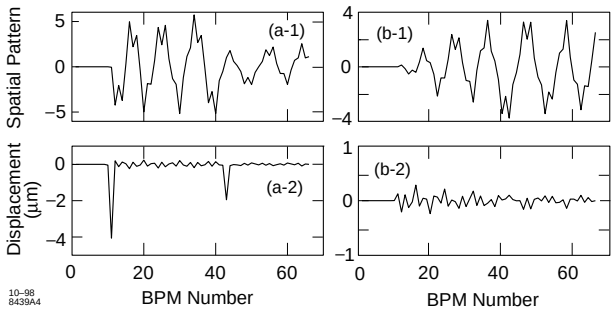

FIG. 4. Typical plots for displacement analysis of physical bases. The top plots show the spatial patterns for random bunch length (a-1) and phase (b-1) variations while the corresponding displacements ($\vec{d}$) are shown in the bottom plots.

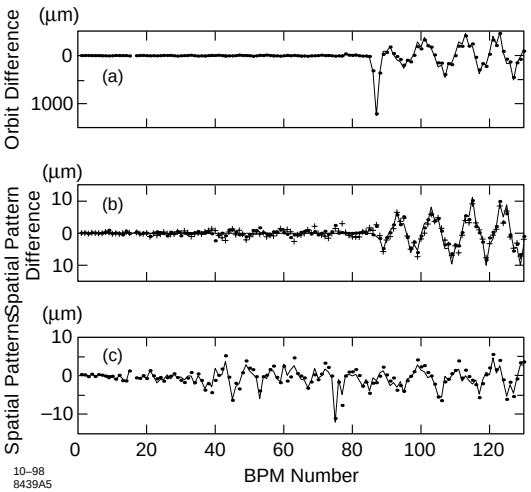

FIG. 5. Transverse wakefield effect measurement in vertical plane for the Stanford Linear Accelerator. The (a) plot shows the average orbit difference with and without a bump introduced on the particle trajectory. The (b) plot shows the difference of the spatial patterns from currently jittering with and without the bump. The (c) plot shows the spatial patterns under nominal conditions.

Using the measured temporal patterns of the current, the corresponding spatial patterns were obtained by applying Eq. (3). Plotted in Fig. 5(b) are the differences in these spatial patterns for sets D2 − D1 (dots) and D2 − D3 (crosses). Since wakefield effects depend strongly on the current, we take the pattern shown as characteristic of the transverse wakefield effect on the beam. This is further supported by the solid curve which shows the theoretical prediction for the effect of a transverse wakefield on the beam. The three curves agree with each other very well. Note that this remarkable result was obtained despite the fact that the signal peak amplitude, less than 10 μm, was comparable to the BPM resolution.

Shown in Fig. 5(c) are the raw spatial patterns for the current sets D1 (dots) and D3 (solid line) taken under nominal conditions. The two spatial patterns match fairly well. Note that the signal amplitude is less than the BPM resolution.

In summary, we have presented model-independent analysis (MIA) techniques for beam line analysis in an accelerator. We have illustrated that the particle centroid motion can be described complementarily in terms of temporal and spatial patterns. In addition, using an SVD we have shown that the number of parameters affecting beam motion can be determined. Combining these two approaches, one is able to resolve the particle trajectory into a superposition of spatial patterns corresponding to the changing physical variables. MIA has many advantages in comparison with other measurement techniques. For example, the resolution of BPMs can be measured directly and improved by using more beam pulses and BPMs; systematic BPM errors can be immediately identified and removed; the BPM noise can be reduced by performing an SVD and setting noise eigenvalues to 0; the primary effects, such as betatron motion, can be identified and separated from the secondary effects; and the locations where the other patterns arise and their corresponding kick strengths can be identified using the degree-of-freedom plot and the displacement representation. Applications to the SLC were presented, including a study of transverse wakefields generated by misaligned structures. This application is of interest for future linear colliders. In general, the concepts presented here are applicable to any system involving a number of sources and a larger number of sensors with unknown correlations.

We wish to point out that MIA is different from the response-matrix method [2,3], although both methods use SVD. MIA does not require a beam line model and is noninvasive or minimally invasive to the accelerator operations. MIA decomposes the trajectory into spatial patterns arising from already present, known or unknown, variables affecting the beam motion. In contrast, the intent of the response-matrix method is to validate or update a machine model, and to do this, purposely activates many sources (correctors). To make sensitive measurements in a linear collider where the beam line is actually changing with time, sometimes dramatically, it is crucial to have a method that does not rely upon or require a reference to a model. However, the two methods are not exclusive and could be integrated.

We thank A. Chao, W. J. Corbett, M. Lee, P. Raimondi, and P. Tenenbaum for valuable discussions and N. Phinney, M. Ross, and the SLAC operations staff for their support in performing the experiments. We also thank S. Smith for useful discussions on his experience in using SVD for studies of random BPM errors. This work was supported by DOE Contract No. DE-AC03-76SF00515.

[1] Gene H. Golub and Charles F. Van Loan, in *Matrix Computations* (The Johns Hopkins University Press, Baltimore, 1996), 3rd ed.

[2] W. J. Corbett, M. J. Lee, and V. Ziemann, in *Proceedings of the 1993 Particle Accelerator Conference* (IEEE, Washington, DC, 1993), p. 108.

[3] J. Safranek, Nucl. Instrum. Methods Phys. Res., Sect. A **388**, 27 (1997).